DOI: 10.1002/ente.201402204

Disposable Heater Arrays Using Printed Silver Patterns on Polyethylene Terephthalate for Multipurpose Applications

Sunil Walia, Ritu Gupta,* and Giridhar U. Kulkarni*[a]

Flexible, semitransparent and robust heating arrays have been designed by grayscale printing as ready-to-use devices for point-of-care application. A perforated Ag mesh is first fabricated with tunable features by controllably varying the toner grayscale value during laser printer on PET. The resistance could be varied between 1 to 2 Ω by tuning the Ag fill factor from 50 to 70%. The Ag/PET heater based on joule heating is able to attain highly stable temperatures upto ~135 °C maintained over long hours. Since temperature is directly related to resistance, this provides a fine temperature knob without any cumbersome processing steps. The merit of design allows individual heating elements to attain stable temperatures at low voltages (~1.5 V) without any interference from neighboring heaters of the array, thus resulting in a thermal library. A laptop USB with 5.1 V output is able to power the thermal library for temperatures in the range of 30–60 °C, useful in many practical applications. It is a multipurpose disposable chip for in-situ transmission microscopy that can be utilized for bioassay and point-of-care diagnostics, as demonstrated in the study.

Introduction

There has been tremendous activity in plastic electronics in recent years, aiming at increasingly simpler fabrication techniques and low cost.[1,2] A device, optoelectronic or non-optoelectronic, can now be realized with all functional components built onto the same plastic chip.[3,4] Much of the impetus for plastic electronics comes from the field of diagnostics.[5] Disposable plastic chips used in a non-clinical, point-of-care setting are highly desirable. Such miniaturized diagnostic techniques[6,7] are advantageous over laboratory testing since rapid analysis can be carried out easily over a small area with low power consumption and small reagent volumes. Furthermore, the quantitative results can be obtained on the field. Multiple functional devices with several working elements such as sensors, heaters, microfluidic channels, energy storage devices can be integrated together on the same chip for combinatorial analysis as well.[8–10] For highly sensitive studies, chips are fabricated clinically on rigid substrates with the state-of-the-art microfabrication process involving multiple steps and expensive materials such as Au and Pt by vacuum evaporation thus making it expensive[11–13] and therefore inaccessible for point-of-care, low cost settings.

We have developed a simple device that can have wide applicability as a heater chip for medical and bio-applications when used as disposable optical microscopy test platform. Whereas one can envision any arbitrary substrate for microscopy measurements, biological microscopy analysis is commonly done in the transmission mode under in-vitro conditions where attaining desired temperatures requires a sophisticated heater stage. In this context, we considered it important to design and fabricate low cost disposable transparent heater array chips which can be operated with simple power supply such as USB (Universal Serial Bus) from a laptop.

Conventionally, transparent heaters find applications in defoggers,[14–16] display, touch-screen panels, camera lenses,[14] transparent sensors[17] and thermochromic displays.[18] These essentially make use of a transparent conductor as a joule heater. While conventionally indium tin oxide (ITO)-based transparent heaters[19,20] have been in use for many years, recently nanomaterials such as metal nanowires,[15] CNTs[14,21,22] and graphene[16,23] are increasingly used in transparent heaters. Large area transparent heaters have been demonstrated based on metal wire networks obtained using crackle lithography.[24,25] However, in the above approaches, either the material is expensive or the process is intensive, and not ideally suited to low cost disposable technology.[26] In a recent work, a simple method using an office laser printer has been shown to work well to produce Ag-based transparent conductors on plastic sheets with controlled fill factor, thereby controlling the optical transmittance and the sheet resistance over wide ranges.[27] In this work, we have explored the use of such

[a] S. Walia, Dr. R. Gupta,[+] Prof. G. U. Kulkarni
Chemistry & Physics of Materials Unit and
Thematic Unit of Excellence in Nanochemistry
Jawaharlal Nehru Centre for Advanced Scientific Research
Jakkur P.O., Bangalore, 560064 (India)
E-mail: ritu.jnc@gmail.com
kulkarni@jncasr.ac.in

[+] Current address:
Birck Nanotechnology Centre
Purdue University
West Lafayette, IN 49707 (USA)

Supporting Information for this article is available on the WWW under http://dx.doi.org/10.1002/ente.201402204.

Part of a Special Issue on "Printed Energy Technologies". To view the complete issue, visit:
http://onlinelibrary.wiley.com/doi/10.1002/ente.v3.4/issuetoc

transparent conductors as transparent heaters for transmission microscopy. Indeed, by controlling Ag fill factor, we have produced arrays of heaters in the form of a chip, covering a desired temperature range. The chip has been used in different contexts as a disposable device.

Results and Discussion

We have prepared perforated Ag mesh by printing grayscale toner on polyethylene terephthalate (PET) with a laser printer, a lithographic recipe developed earlier by us.[27] Briefly, a design of desired grayscale toner was printed on PET sheet using a laser printer (Figure 1a). The Ag ink (~200 µL for $3\times3\,cm^2$) was coated all over the grayscale-printed PET, heated to 135 °C to decompose the Ag precursor followed by removal of toner by toluene, resulting in a perforated Ag mesh (Figure 1b). Since the resulting perforated Ag mesh is a replica of the toner pattern printed on the substrate, the toner essentially acts as a negative resist. The grayscale design (size and spacing between the toner dots) vary from printer to printer, the fill factor of toner with respect to defined gray scale was optimized for a given printer (Figure 1c). The toner grayscale was between 15 to 30%, such that the dots were placed a minimum distance apart without touching each other and the replica Ag exhibited good connectivity. The Ag metal coverage (also called Ag fill factor) and toner fill factor were calculated using image J software. The Ag metal coverage is directly related to the toner fill factor which is varied between 30–50% for grayscale of 15 to 30%. A toner grayscale value of 15% resulted in perforated Ag mesh with holes of 125 µm and mesh width of ~85 µm, while the 30% value of grayscale increased Ag holes to 190 µm (Figure 1d). Beyond 30% grayscale, the Ag mesh pattern became discontinuous and non-uniform. The resistance and transmittance of perforated Ag mesh fabricated by different grayscale printing (15–30%) is shown in Figure 2a. The Ag meshes are highly conducting with resistance varying between 1–2 $\Omega\,\square^{-1}$, while the transmittance is expectedly low (25–45%) due to higher Ag coverage. Figure 2b(top) shows an original photograph of a strip of Ag meshes obtained by using different grayscale values (15 to 30%) during printing on PET (substrate marked by dotted lines) separated by continuous Ag film (contact pad) with bottom illumination. The printed Ag mesh electrodes were joule heated by applying a voltage of 1.5 V across the stripe. The corresponding thermal image is shown in Figure 2b(bottom). As can be seen from the thermal image, the different Ag mesh regions attained different saturated temperatures for a given current. This is because of different extents of joule heating due to the difference in their resistances as shown in Figure 2a. The Ag mesh with highest resistance acquired highest temperature and vice versa. Importantly, the joule heat produced in the heater is localized in the printed Ag region because of the thermally insulating

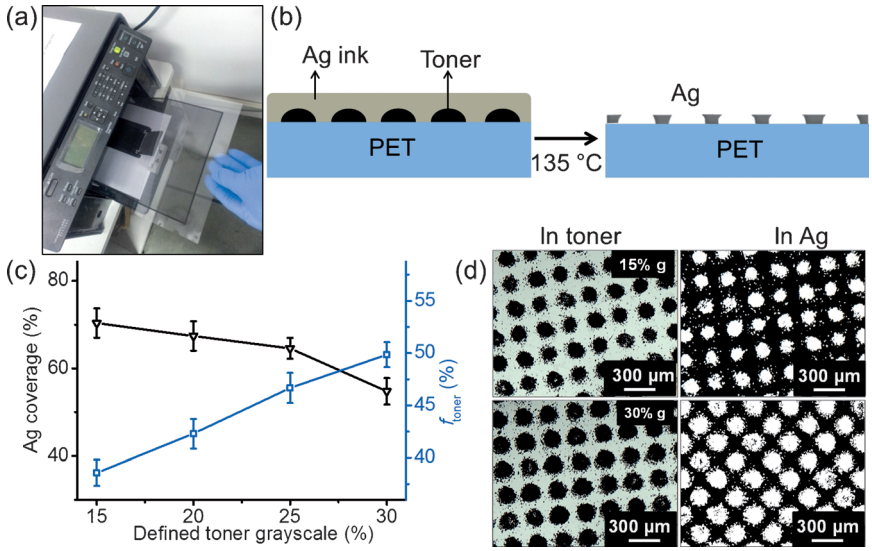

Figure 1. a) A photograph showing printing of grayscale design on PET sheet. b) Schematic demonstrating the process steps involved in the fabrication of Ag electrodes. c) Ag coverage and toner fill factor variation with respect to defined toner grayscale. d) Optical photographs of printed patterns in toner (left) and corresponding perforated Ag mesh (right) with grayscale of 15% and 30%.

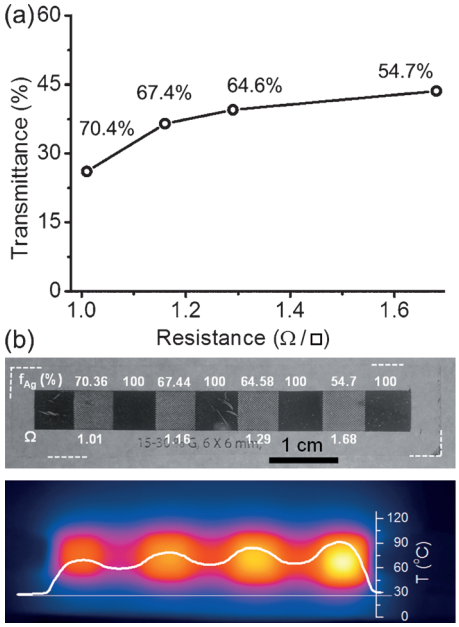

Figure 2. a) Relationship between sheet resistance and transmittance for perforated Ag mesh. The values shown in % are the Ag fill factors. b) Photograph of a Ag-developed grayscale pattern with defined grayscale of 15, 20, 25, and 30% printed together as a chip and the corresponding thermal image.

nature of PET sheet. The temperature profile across the electrode stripe is shown overlaid with the thermal image in Figure 2b(bottom). This essentially acts as a heater array with 4 heating zones, which we termed as a thermal library. In the designed heaters, Ag mesh regions are connected by continuous Ag stripe (predefined in the CAD file; see Figure S1), Thus, for the electric contacts between the Ag mesh heater zones, no extra step of printing contact pads was required which is usually done in a following step by screen printing metal paint/ink or such techniques. This is an additional advantage of this technique since making good ohmic contacts without any resistive loss is very important for heater applications.

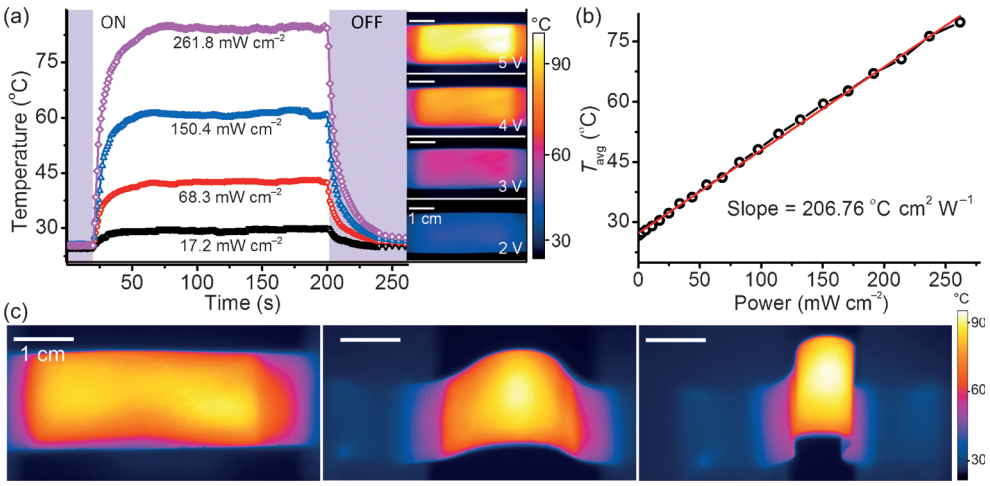

Figure 3. Fabrication of perforated Ag-mesh-based (~70% Ag coverage) heater. a) Rise and fall temperature curves at applied voltages of 2, 3, 4, and 5 V and the corresponding thermal images. b) Plot of average temperature with respect to power per unit area. c) Thermal images demonstrating flexibility of the heater operating at 5 V.

The heating performance of the Ag mesh was studied in detail. As seen from the temperature profiles at different applied voltages, Ag mesh exhibits a fast response time of ~30 s as shown in the temperature profile of Figure 3a. The power indicated is calculated per unit area from the product of applied voltage and current passing through the Ag pattern that acts as resistor. As expected, the temperature achieved is higher at higher power. The heating and cooling rates derived from the first derivative of the temperature rise and fall curve of the heater is ~7 °C s^{-1} at 261.8 mW cm^{-2} (see Figure S2). As seen from the thermal images in Figure 3a, the steady state temperature is uniformly distributed across the patterned area with a temperature fluctuation of ±0.7 °C in ambient conditions. The uniform temperature distribution is achieved due to the uniformity in grayscale printing of the toner and of Ag in the subsequent step. The power required per centimeter square area for raising the temperature from room temperature to ~85 °C is 261.8 mW cm^{-2}. The power values are noticeably low as indicated by the thermal resistance obtained from the slope, 206.76 °C cm^2 W^{-1}. Since the Ag mesh is supported on flexible substrate (PET), the heater is also flexible in nature (Figure 3c). The heater temperature was set to approximately 95 °C by applying 5 V with the two ends of the heater supported between the movable clamps in flat position (Figure 3c, left). As the two ends were brought closer for flexing, the thermal images were taken as shown (Figure 3c). The temperature remained almost unaffected even for repeated bending cycles. This clearly demonstrates that the resistance does not change with flexing. Since the flexible heater is mechanically robust, it can be used as a flexible hot stage.

With regards to heater performance, we have examined three aspects, long term stability, control over temperature and temperature-live microscopy, the last one for the purpose of demonstrating the concept of a thermal library to perform temperature-based combinatorial studies. The long term stability of the heater is crucial for its practical application. This parameter was tested by carrying out a solid state reaction over extended hours. The chosen reaction has previously been used for the synthesis of Au microplates,[28] where temperature stability is required. The schematic in Figure 4a shows the experimental setup for the synthesis of Au micro-

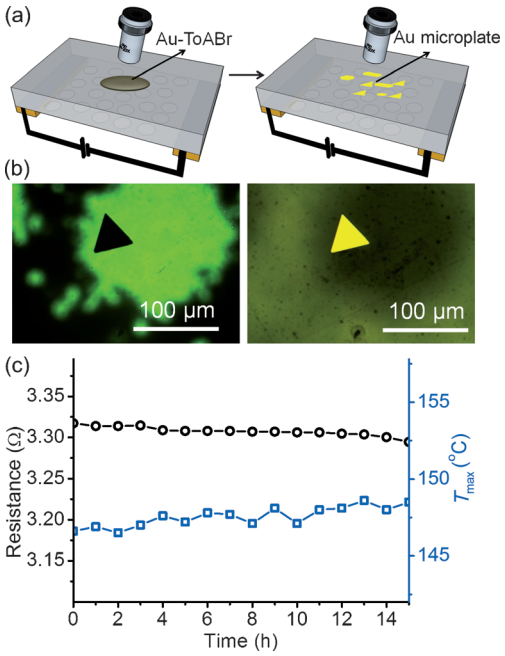

Figure 4. Ag-mesh-based heater as in-situ heating stage for microscopic growth study. a) Schematic demonstrating the synthesis of Au microplate from the Au–organic precursor by in-situ heating under direct transmission microscope. b) The growth of Au microplate on PET substrate with integrated Ag-mesh-based heater observed in transmitting (left) and reflecting mode (right). c) The change in resistance and maximum temperature with time while heater is operated at constant voltage of 0.7 V.

plates on the Ag-mesh-based heater while the growth process is observed in-situ with the microscope. The perforated Ag mesh heater ($6 \times 6\ mm^2$) was joule heated by applying 0.7 V to raise the temperature up to 150 °C, sufficient for decomposition of the Au–organic precursor (see Experimental Section).[28] Figure 4b shows the optical photograph of an isolated microplate synthesized on the Ag mesh heater, both in transmitting and reflecting mode, taken from the same region after 14 h of reaction. The transmitting mode imaging was possible, firstly because the perforated mesh is semi-transparent and secondly, the object of interest can be kept in focus without interference from the heater mesh as the latter would be out of focus at the back of PET layer. As seen in Figure 4bfor moderate thickness of PET, the perforated mesh is blurred while the focus is on the microplate. The blurred mesh in the background, if perceived as a hindrance, can be completely taken away from the view by increasing the thickness of the PET substrate or encapsulating the heater with a diffuser layer.

As seen in Figure 4c, the heater resistance change is minimal with a negligible change in set temperature even after heating for 14 h. This demonstrates the stability of the heater makes it appropriate for such long time-scale studies.

For any thin film heater, temperature control and calibration are important aspects. In the present case, these aspects were addressed by temperature-based florescent confocal imaging of Rhodamine 6G films coated onto the PET side of grayscale printed Ag mesh heaters. Fluorescent dyes e.g, Rhodamine 6G, Rhodamine B, Rhodamine 110, etc.[29–32] have been used previously as surface temperature probes. Figure 5a shows average florescent intensity (measured from the image of R6G film as shown in inset of Figure 5a) at different set temperatures. The applied power is calibrated using an IR camera for determining accurate temperature values (Figure S3). The temperature of the R6G film/heater was raised by joule heating (Figure S3). As seen from the plot, the relative fluorescence intensity (with respect to intensity at room temperature) decreases on heating, possibly due to aggregation of dye molecule.[33] Figure 5bshows switching of florescent intensity with time at applied power of 0 and 60 $mW\,cm^{-2}$, which corresponds to temperatures of 25 and 36 °C, respectively. The intensity decreases rapidly in correspondence with the thermal and the confocal images (Figure 5b and Figure S4). The time required for intensity and temperature is almost equal at a given power. This provides an optical readout of temperature of the heater surface without any need for thermal imaging during in situ biological studies. This can be an extremely useful tool for measuring temperatures at solid surface as well as in liquid phase.

A 3×3 array of Ag-based heaters connected in series is designed to create a thermal library for combinatorial studies (Figure 6a). For point-of-care applications, the assembly is powered with a commonly available laptop USB capable of giving an output voltage of 5.1 V. Since the total resistance of the heater is rather low (~50 Ω), a low voltage source suffices (Figure 6a). Figure 6b is a digital photograph of the thermal library with 32 heating zones divided into 8 strips

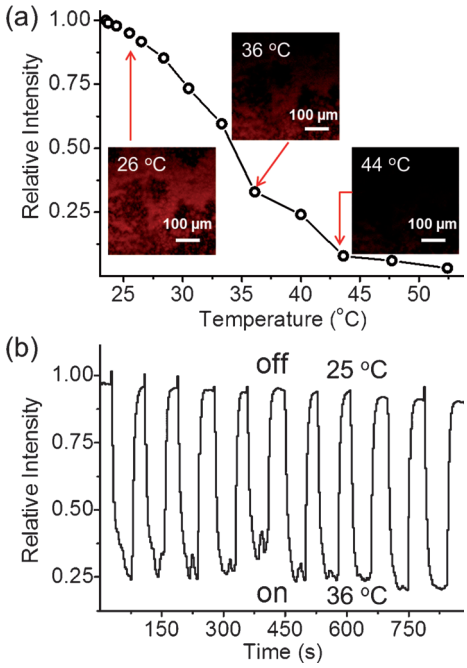

Figure 5. Temperature-dependent-fluorescence study of R6G using confocal microscopy. a) The change in the florescence intensity on heating the R6G film coated on PET hosting Ag mesh heater on the other side. Insets are the confocal images for 3 different temperatures. b) The reversible fluorescent intensity changes by switching the heater on and off.

(each strip was printed using grayscale value of 15, 20, 25, and 30%). The temperature range of 30–60 °C is achieved, which is of biological interest. As demonstrated, the stability of the laptop as a power source is appreciable when compared to a standard power source at the applied voltage of 5.1 V (Figure 6c and d). The temperature achieved is different for different grayscales, as expected. Heaters with similar grayscale values may also show slight variation, possibly due to printing defects. However, one can always refer to an accompanying data sheet of a thermal library with specified temperatures for practical purposes. The temperature attained by different heating zones of the thermal library, essentially follows the trend of resistance (Figure S5), indicating negligible crosstalk among the zones.

Temperature-dependent live microscopy is a strong tool in research for examining biological samples.[34–36] In general, such microscopy is not done in real time as the specimen needs to be fed into a hot stage while imaging. Below is shown a study of live erythrocytes (red blood cells, RBCs) in real time while heating over the Ag mesh heater. Figure 6e is the schematic of experimental setup for RBCs imaging. The polydimethylsiloxane (PDMS) well was made on the back side of the grayscale-printed heater as shown in Figure 6e. The RBCs were taken from a healthy human volunteer and the serum was diluted 100 times in 0.9% isotonic solution of NaCl. A drop of 20 µL of this solution containing RBCs was placed inside the PDMS well. The optical image was taken in transmitting mode while cells were at room temperature (Figure 6f). The temperature of the heater was

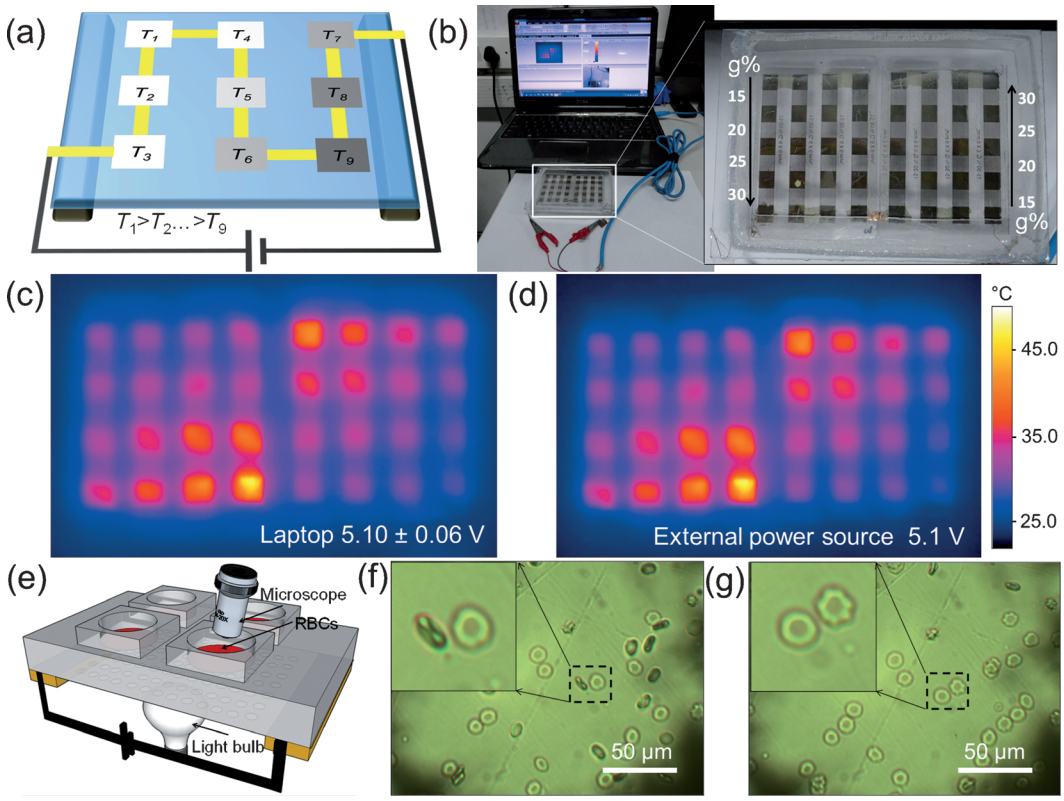

Figure 6. Thermal library. a) Schematic showing addressable printed resistors connected to a common power source. b) Photograph showing the portable thermal library powered by laptop. The thermal image of addressable printed resistors at 5.1 V while connected to (c) laptop as power source and (d) external power source. Red blood cells imaging: e) Schematic diagram of the experimental setup for RBCs imaging. The optical photograph of RBCs, (f) before and (g) after heat treatment. Inset shows magnified images of the same cells before and after heating.

raised to approximately 50 °C by joule heating and RBCs were examined in real time. As can be seen by the optical image in Figure 6 f and g, the bi-concave-shaped cells became irregular upon heating. The use of temperature-based in-situ monitoring on living cells (e.g. cancers cells) are of great interest. There are several other biological applications as well that require heating at low temperatures below 90 °C for example, polymerase chain reaction studies (PCR), cell growth, etc.[37,38] Thus, elucidation of temperature effect on the life span of the living cell and monitoring them in real time can reveal many important aspects relevant to diseases, particularly in the context of point-of-care applications.

Conclusions

We have used a laser-printed template for the fabrication of perforated Ag-film-based semi-transparent heaters. This has served as a low cost, fast technique for printing on a flexible substrate such as PET. By controlling the Ag fill factor based on grayscale printing, we have been able to tune the resistance and thus the heating behavior of the resulting heater. This is indeed a disposable heater array as the cost would be very low (~$0.20) as the ingredients (particularly Ag) are used in very small quantities and are benign to the environment. By printing an array of heaters with varied Ag fill factors, we have produced thermal libraries for combinatorial studies. Recycling Ag would add to the cost and may not be viable. After having examined the stability of the produced heaters for many hours in a slow solid-state reaction involving Au microplate growth, the temperature cycling was studied using a fluorescent probe (R6G). We have also utilized the heater in transmission mode to show its usage as hot stage in combination with microscopy for biological specimens. The disposability imparts an additional advantage as it can be used in the context of diagnostics where reusability requires stringent sterilization processes. This multipurpose disposable chip should prove to be a disruptive technology for point-of-care applications.

Experimental Section

Fabrication of grayscale electrodes

The grayscale patterns were designed using Adobe Illustrator software (CS6 version) and printed on PET (Melinex ST-506, DuPont) using a Xerox WorkCentre 5230 laser printer with a printing resolution of 600 dpi (black/white mode). In grayscale, 100 % gray represents black and 0 % gray stands for no print (white). The Melinex sheets from DuPont were selected due to their superior mechanical, thermal, and modified adhesion properties. The Ag precursor ink (Inktec PR010) is purchased from Inktec, Korea and used as supplied.

Fabrication of heaters

Different grayscale designs were made with Ag for semi-transparent microheaters. The electrode contacts were established using thick epoxy Ag paint. The substrate was mounted for imaging with supports at both ends such that the patterned area is kept hanging in air while the imaging is done from the back side of the patterned area. The voltage was applied using an external power source (Keithley 2400) as well as using a USB powered by a laptop. Thermal imaging was carried out using Testo thermal imager (Testo 885). The images were analyzed using offline software.

Characterization

Optical microscope (Laben, India) was used for capturing images and measurements. The image analysis was performed using Image J software for calculating toner and Ag fil factor. Surface profilometry was carried out using a contactless, 3D, white light interferometer (Veeco Wyko NT9100). SEM imaging was done using Nova NanoSEM 600 instrument (FEI Co., The Netherlands). XRD measurement was done using Bruker diffractrometer employing CuK_{α} ($\lambda = 1.5406$ Å) radiation. TGA analysis was carried out with a Mettler Toledo Star instrument (Weinheim, Germany). Low temperature resistivity measurements were done using THMS600 stage (Linkam Scientific Instruments Ltd., UK). The transmittance of the film was measured in specular and diffuse mode using PerkinElmer Lambda 900 UV/visible/near-IR spectrophotometer with integrated sphere. Sheet resistance was measured using a custom-designed 4-point probe station.

Temperature dependent fluorescence measurements

Rhodamine 6G (R6G) solution in ethanol (0.4 mg mL^{-1}) was drop coated on the back side of Ag/PET thermal heater supported in a hollow frame. The fluorescent images were recorded with 10× zoom in the reflecting mode using a laser scanning confocal microscope (Zeiss LSM-510) with a excitation wavelength of 488 nm (power 30 mW, 1% illumination) at single incident and emission angle. The field of view (450μm × 450 μm) was kept unchanged for measuring the relative changes in temperature-dependent intensity of R6G fluorescence. For intensity measurement, the fluorescent maps were imported in image J software and average intensity was calculated over the entire image area.

Synthesis of Au microplates

Gold tetraoctylammonium bromide (Au–ToABr) (50 mM in toluene) solution was prepared using phase-transfer reaction between hydrogen tetrachloroaurate(III) hydrate, tetraoctylammonium bromide (ToABr), and toluene (obtained from Sigma–Aldrich and used without further purification). Then 50 μL of this solution was drop-coated onto Ag mesh heater. Finally temperature was raised up to 150 °C by joule heating and synthesis of Au microplates was carried out for the next 14 h.

Temperature-dependent imaging of RBCs

The blood was taken from healthy human body using doctorate syringe. Then it was diluted in 0.9% of NaCl solution. Finally, 20 μL of this solution was taken and drop coated onto the heater for in-situ imaging RBCs. After drop coating the solution Ag mesh heater was joule heated and the change in cell shape was examined using optical microscope (Laben, India).

Acknowledgements

The authors are grateful to Professor C. N. R. Rao for his encouragement. The financial support from the Department of Science and Technology, Government of India, is gratefully acknowledged. R.G. acknowledges JNCASR for postdoctoral fellowship. S.W. acknowledges CSIRfor fellowship.

Keywords: Ag pattern · combinatorial chemistry · conductive materials · point-of-care · thermal library

[1] D. Hohnholz, H. Okuzaki, A. G. MacDiarmid, *Adv. Funct. Mater.* **2005**, *15*, 51–56.
[2] J. Huang, G. Li, Y. Yang, *Adv. Mater.* **2008**, *20*, 415–419.
[3] D.-H. Kim, N. Lu, R. Ma, Y.-S. Kim, R.-H. Kim, S. Wang, J. Wu, S. M. Won, H. Tao, A. Islam, K. J. Yu, T.-i. Kim, R. Chowdhury, M. Ying, L. Xu, M. Li, H.-J. Chung, H. Keum, M. McCormick, P. Liu, Y.-W. Zhang, F. G. Omenetto, Y. Huang, T. Coleman, J. A. Rogers, *Science* **2011**, *333*, 838–843.
[4] G. Gruner, *J. Mater. Chem.* **2006**, *16*, 3533–3539.
[5] A. Bhattacharyya, C. M. Klapperich, *Anal. Chem.* **2006**, *78*, 788–792.
[6] G.-B. Lee, S.-H. Chen, G.-R. Huang, W.-C. Sung, Y.-H. Lin, *Sens. Actuators B* **2001**, *75*, 142–148.
[7] Y. S. Shin, K. Cho, S. H. Lim, S. Chung, S.-J. Park, C. Chung, D.-C. Han, J. K. Chang, *J. Micromech. Microeng.* **2003**, *13*, 768.
[8] H. Andersson, A. van den Berg, *Lab Chip* **2004**, *4*, 98–103.
[9] E. Traversa, *Sens. Actuators B* **1995**, *23*, 135–156.
[10] M. Kaltenbrunner, T. Sekitani, J. Reeder, T. Yokota, K. Kuribara, T. Tokuhara, M. Drack, R. Schwödiauer, I. Graz, S. B. Gogonea, S. Bauer, T. Someya, *Nature* **2013**, *499*, 458.
[11] S. Claramunt, O. Monereo, M. Boix, R. Leghrib, J. D. Prades, A. Cornet, P. Merino, *Sens. Actuators B* **2013**, *187*, 401–406.
[12] G. Xiong, C. Meng, R. G. Reifenberger, P. P. Irazoqui, T. S. Fisher, *Energy Technol.* **2014**, *2*, 897–905.
[13] R. Gupta, R. G. Reifenberger, G. U. Kulkarni, *ACS Appl. Mater. Interfaces* **2014**, *6*, 3923–3929.
[14] Y. H. Yoon, J. W. Song, D. Kim, J. Kim, J. K. Park, S. K. Oh, C. S. Han, *Adv. Mater.* **2007**, *19*, 4284–4287.
[15] T. Kim, Y. W. Kim, H. S. Lee, H. Kim, W. S. Yang, K. S. Suh, *Adv. Funct. Mater.* **2013**, *23*, 1250–1255.
[16] D. Sui, Y. Huang, L. Huang, J. Liang, Y. Ma, Y. Chen, *Small* **2011**, *7*, 3186–3192.
[17] H. Choi, J. S. Choi, J.-S. Kim, J.-H. Choe, K. H. Chung, J.-W. Shin, J. T. Kim, D.-H. Youn, K.-C. Kim, J.-I. Lee, S.-Y. Choi, P. Kim, C.-G. Choi, Y. J. Yu, *Small* **2014**, *10*, 3685–3691.
[18] R. Gupta, S. Walia, M. Hösel, J. Jensen, D. Angmo, F. C. Krebs, G. U. Kulkarni, *J. Mater. Chem. A* **2014**, *2*, 10930–10937.
[19] K. Im, K. Cho, J. Kim, S. Kim, *Thin Solid Films* **2010**, *518*, 3960–3963.
[20] K. Im, K. Cho, K. Kwak, J. Kim, S. Kim, *J. Nanosci. Nanotechnol.* **2013**, *13*, 3519–3521.
[21] Z. P. Wu, J. N. Wang, *Physica E* **2009**, *42*, 77–81.
[22] D. Jung, D. Kim, K. H. Lee, L. J. Overzet, G. S. Lee, *Sens. Actuators B* **2013**, *199*, 176–180.
[23] J. Kang, H. Kim, K. S. Kim, S. K. Lee, S. Bae, J. H. Ahn, Y. J. Kim, J. B. Choi, B. H. Hong, *Nano Lett.* **2011**, *11*, 5154–5158.
[24] R. Gupta, K. D. M. Rao, K. Srivastava, A. Kumar, S. Kiruthika, G. U. Kulkarni, *ACS Appl. Mater. Interfaces* **2014**, *6*, 13688; K. D. M. Rao, R. Gupta, G. U. Kulkarni, *Adv. Mater. Interfaces* **2014**, *1*, 1400090.
[25] S. Kiruthika, R. Gupta, K. D. M. Rao, S. Chakraborty, N. Padmavathy, G. U. Kulkarni, *J. Mater. Chem. C* **2014**, *2*, 2089; S. Kiruthika,

K. D. M. Rao, A. Kumar, R. Gupta, G. U. Kulkarni, *Mater. Res. Express* **2014**, *1*, 026301.
[26] G. Xiong, C. Meng, R. G. Reifenberger, P. P. Irazoqui, T. S. Fisher, *Electroanalysis* **2014**, *26*, 30–51.
[27] R. Gupta, M. Hösel, J. Jensen, F. C. Krebs, G. U. Kulkarni, *J. Mater. Chem. C* **2014**, *2*, 2112–2117.
[28] B. Radha, G. U. Kulkarni, *Cryst. Growth Des.* **2011**, *11*, 320–327.
[29] T. Kan, H. Aoki, N. Binh-Khiem, K. Matsumoto, I. Shimoyama, *Sensors* **2013**, *13*, 4138–4145.
[30] J. Vogt, P. Stephan, *Meas. Sci. Technol.* **2012**, *23*, 105306.
[31] P. Löw, B. Kim, N. Takama, C. Bergaud, *Small* **2008**, *4*, 908–914.
[32] K.-H. Yang, F.-D. Mai, C.-C. Yu, Y.-C. Liu, *Analyst* **2014**, *139*, 5164–5169.
[33] A. Pucci, R. Bizzarri, G. Ruggeri, *Soft Matter* **2011**, *7*, 3689–3700.
[34] D. P. Allison, N. P. Mortensen, C. J. Sullivan, M. J. Doktycz, *WIREs Nanomed Nanobiotechnol* **2010**, *2*, 618–634.
[35] C. L. Rieder, A. Khodjakov, *Science* **2003**, *300*, 91–96.
[36] D. J. Stephens, V. J. Allan, *Science* **2003**, *300*, 82–86.
[37] Y. Yu, B. Li, C. A. Baker, X. Zhang, M. G. Roper, *Anal. Chem.* **2012**, *84*, 2825–2829.
[38] J. L. Lin, M.-H. Wu, C.-Y. Kuo, K.-D. Lee, Y.-L. Shen, *Biomed. Microdevices* **2010**, *12*, 389–398.

Received: December 12, 2014
Revised: February 7, 2015
Published online on April 7, 2015